THE EFFECTS OF NON-METALLIC INCLUSIONS ON MECHANICAL PROPERTIES AND PERFORMANCE OF STEEL

Kip O. Findley*, E.B. Damm
*Colorado School of Mines
Metallurgical and Materials Engineering
1500 Illinois St.
Golden, CO, 80401
e-mail: kfindley@mines.edu

EXECUTIVE SUMMARY

This paper describes the effect of inclusions on the mechanical properties and performance of steels. Inclusion thermophysical properties and the nature of the interface between the inclusion and steel play is important for steel performance. During deformation and fracture, inclusions can serve as nuclei for microvoids or cleavage facets, thereby impacting ductility and fracture energy. In fatigue loading, inclusions can act as crack nucleation sites, depending on the steel strength level, and affect fatigue crack growth resistance. When hydrogen is present in steel, inclusions are large binding energy trap sites, and hydrogen can facilitate void nucleation, thus reducing ductility. Hydrogen that gathers at inclusions also promotes hydrogen induced cracking in pipeline steels. Deformable inclusions can, however, have a beneficial effect on machinability as they lower local fracture resistance for chip formation. This paper also provides a list of references where more detail can be found about the mechanical behavior presented in this paper as well as other properties.

INTRODUCTION

Inclusions are inherent in steel due to the nature of the steelmaking process. There are differences in physical and chemical properties between steel and inclusions, accounting for the effects that inclusions have on steel performance. At the steel-inclusion interface, there is a discontinuity in composition, crystal structure, bond type, coefficient of thermal expansion, and mechanical properties, and thus inclusions have a prominent role in mechanical properties such as fracture, fatigue, hydrogen embrittlement, and machinability. This paper will provide an overview of the effects of inclusions on these properties.

Inclusion types can be categorized as indigenous or exogenous. Indigenous inclusions are present as a result of purposeful additions and chemical reactions occurring during steelmaking, while exogenous inclusions are as a result of unintentional introduction of foreign materials. Common indigenous inclusions found in steels include manganese sulfides, silicates, and oxides. A broad range of exogenous inclusions can also be found in steels as the result of slag entrainment or entrainment of steelmaking refractories or mold release powders for example. The details of how each type of inclusion evolves have been described in detail elsewhere in this volume[1].

DEFORMABILITY OF INCLUSIONS

During the hot working process, individual inclusions and inclusion clusters are either deformed or fractured and dispersed depending on the inclusion plasticity. Figure 1 shows a schematic of the cast and rolled morphology of various types of inclusions[2]. Inclusions that have little to no plasticity at hot working temperatures include Al_2O_3, calcium aluminates, silica, and spinels[3]. Clusters of inclusion particles are broken up and separated during hot working, resulting in oxide stringers elongated in the rolling direction. Individual hard oxide particles or as particles within a stringer often exhibit voids in the leading and trailing ends in the rolling direction of the inclusion as illustrated in Figure 1. Large globular oxide particles are more susceptible to the formation of these voids. Figure 2 shows an example of the formation of these voids in hot rolled steel.

MnS, CaS, and silicates as well as rare earth sulfides and oxysulfides exhibit generally higher plasticity compared to oxides which allows them to be deformed during the hot working process. The index of deformability[4], ν, can be used to quantify the relative level of plasticity of an inclusion with respect to the steel. This index is defined as:

$$\nu = \frac{2 \cdot \log \lambda}{3 \cdot \log h} \qquad \text{Eqn. 1}$$

Where λ is a measure of the minor and major axis of the inclusions ellipsoid, a and b ($\lambda = a/b$), after rolling and h is the as cast cross section area, a_0, divided by the as rolled cross sectional area, a_f.

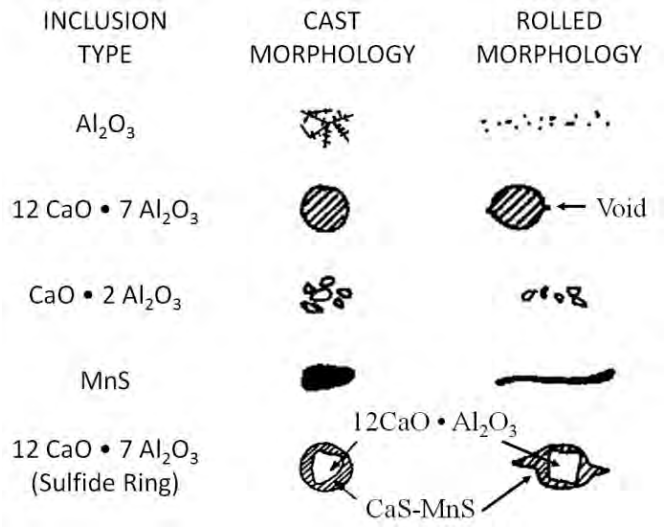

Figure 1: Morphology of as cast and hot rolled inclusions[2].

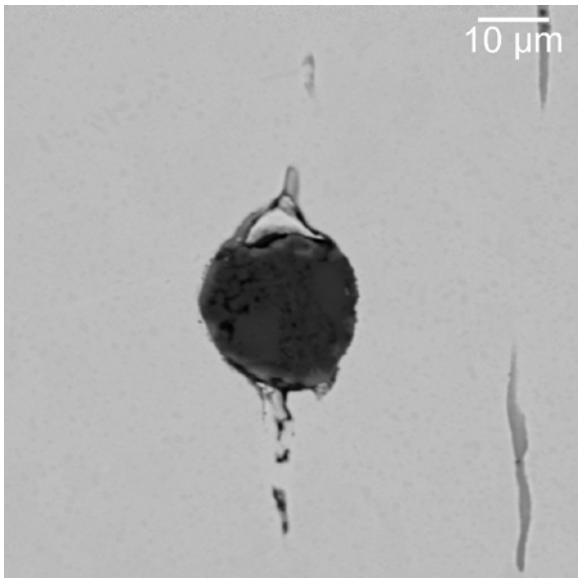

Figure 2: Light optical micrograph of void initiation around an oxide inclusion.

Inclusions with a *v* of nearly 1 elongate significantly, while inclusions that do not elongate exhibit *v* approaching 0 and tend to fracture rather than elongate. Alloy elements can be dissolved in inclusions, affecting their flow stress and plasticity and hence have subtle effects on the index of deformability. Perhaps the more significant effects come from the temperature at which hot working is performed. Duplex inclusions form when CaS-MnS precipitates on hard oxide particles. These inclusions exhibit a deformed outer shell around the hard particle in the as rolled condition.

The index of deformability is evaluated after a given hot working operation and can be used to assess the differences between clusters of hard inclusions which tend to break up in to strings of particles with steel between them, and soft inclusions which tend to primarily elongate. When considering inclusion morphology it is often important to consider the deformation processing path. For example, consider a deformable inclusion in a rolled plate with the orientation shown in Figure 3a. After rolling, the inclusion and elongates and pancakes, and the apparent inclusion size is dependent on the plane of observation as shown in Figures 3b-d. Thus, some mechanical properties are dependent on the orientation of the applied load with respect to the orientation of the pancaked and elongated inclusions. Another example is in forging, where inclusions are affected by forging flow and the formation of the forging flash. Alloying elements such as Ca can be used to reduce the amount of elongation that occurs in soft inclusions such as MnS, thus decreasing anisotropy in mechanical properties.

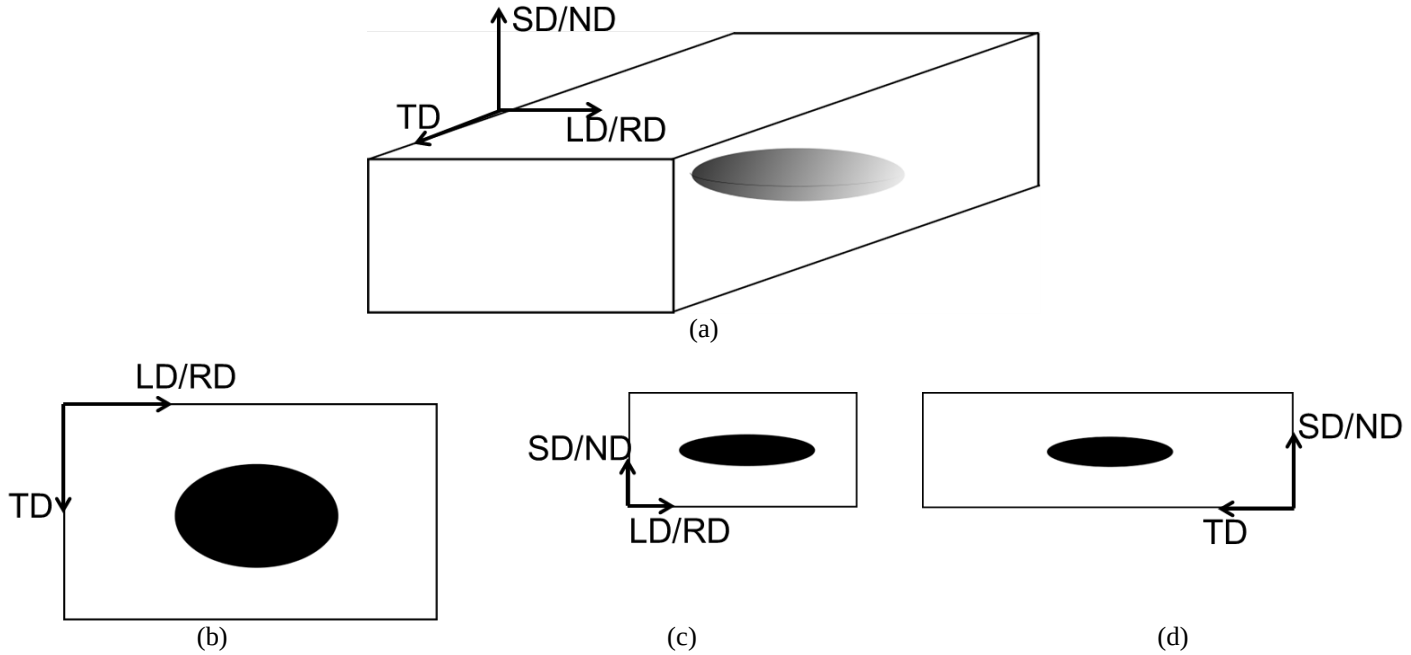

Figure 3: a) Schematic of an inclusion in a rolled plate; (LD: longitudinal direction, RD: rolling direction, TD: transverse direction, SD: short transverse direction, ND: normal direction). b) Inclusion as observed on the TD-LD/RD plane. c) Inclusion as observed on the SD/ND-LD/RD plane. d) Inclusion as observed on the SD/ND-TD plane.

The difference in thermo-physical properties between inclusions and steel may play an important role in steel performance. Many authors point to the difference in the average thermal expansion coefficient between the steel matrix and the inclusion particle as a source for generation of stresses, or even de-bonding during cooling from rolling or thermal treatments. If there are no phase transformations in the temperature range of interest, then differences in coefficient of thermal expansion can result in radial or circumferential residual stresses at the steel-inclusion interface[5]. Thermal expansion coefficients for many oxide inclusions are reported to be in the $8x10^{-6}$ to $13x10^{-6}$/°C range, while values of approximately $18X10^{-6}$/°C are reported for sulfides[5]. When austenite (steel) cools, it contracts at a rate of approximately $23x10^{-6}$/°C, but then during phase transformation steel exhibits a considerable expansion, which is not considered in the previous analysis. Figure 3 illustrates this point. Dilation curves are shown for a series of 86XX steels where XX represents a range of carbon contents in a carburized case. Lines showing linear thermal contractions are included for representative inclusions with thermal expansion coefficients of $8x10^{-6}$, $13x10^{-6}$, and $18x10^{-6}$/°C. A tensile stress may be generated in the austenite during cooling before the transformation temperature, but the expansion associated with the transformation promotes a compressive residual stresses in the matrix in the region of an inclusion. These discussion points do not consider anisotropy or plasticity in the matrix or the inclusions.

THE EFFECTS OF INCLUSIONS ON DUCTILITY AND FRACTURE

Inclusions have a critical impact on tensile ductility and toughness of steel. Most importantly, inclusions are prominent sites for microvoid initiation in regions of a triaxial stress state, as is found in the necked region of a tensile specimen and the notched region of a Charpy impact specimen for example. Inclusions are regions of discontinuity with the ductile steel and can be considered large stress concentrators in the steel matrix. There are other discontinuity features such as grain boundaries and precipitates that are present in larger volume fractions, but their sizes and associated stress concentrations are typically much smaller. Thus, ductile overload fracture surfaces contain large voids that are reflective of the inclusion size distribution along with smaller voids in between. Figure 4 shows fracture surfaces from a 0.3 wt. pct carbon Cr-Mo-Ni steel with alloys and heat treatments designed to have different populations of nitrides[6]; specifically, the conditions contain either mixtures of titanium or zirconium nitrides, or they contain aluminum nitrides. The different void size resulting from these different inclusion populations is apparent.

Both inclusion size and spacing are important characteristics for ductile fracture. A simple proportionality between tensile ductility and these characteristics is:

$$\varepsilon_f \propto 2\ln\left(\frac{L}{w}\right) \qquad \text{Eqn. 2}$$

Where L is the inclusion spacing and w is the inclusion size. Alternatively, fracture strain can be related to inclusion volume fraction as this quantity is inversely proportional to L/w. The amount of uniform strain in tension before necking is not dependent on the inclusion population unless inclusions provide strength to the alloy; however, total strain and reduction in area are dependent on the

inclusion population as ductile damage nucleates and grows during necking. A fracture mechanics approach can be used to show the same effect of inclusion spacing, size, and volume fraction on toughness[7,8], and these inclusion characteristics also impact hot ductility, e.g. during hot working[9].

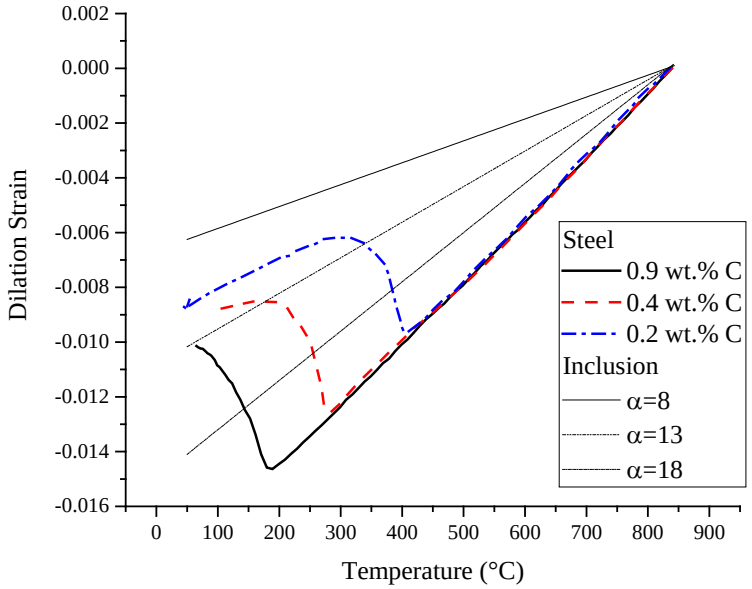

Figure 3: Dilation strain measured for 3 different carbon contents of 86XX series steel compared to linear contraction of inclusions with thermal expansion coefficients of 8, 13, and 18 (x10^{-6})/°C. The expansion in the steel at lower temperatures is due to the austenite to martensite phase transformation.

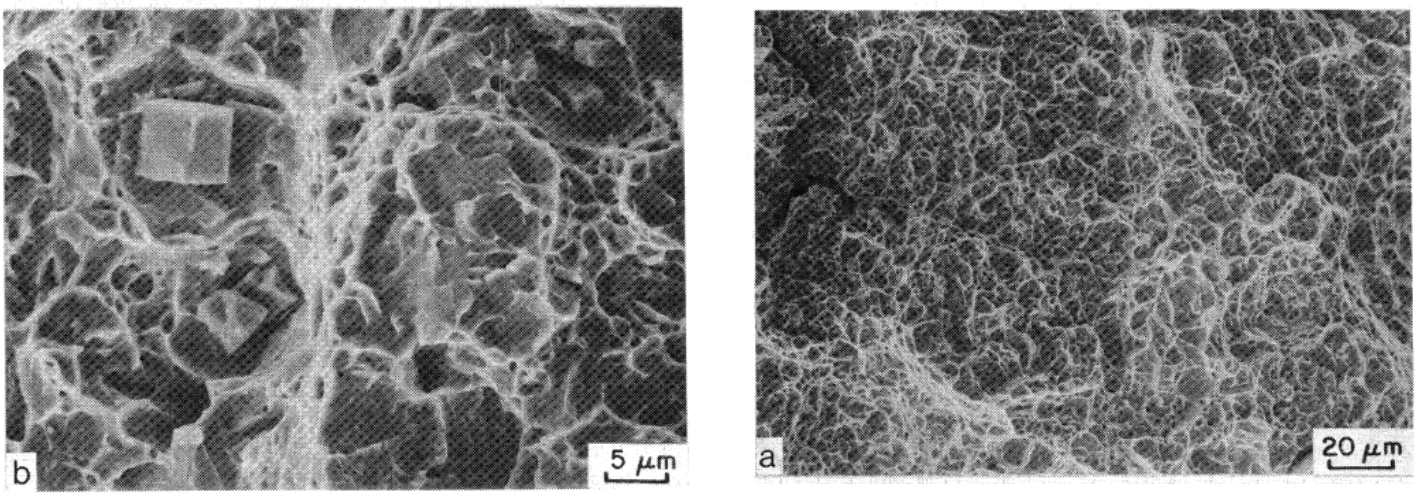

(a) (b)

Figure 4: a) Microvoids reflective of initiation around titanium and zirconium nitrides and b) a population of smaller microvoids reflective of initiation around smaller aluminum nitrides[6].

The Charpy upper shelf energy, which is indicative of alloy toughness under ductile fracture conditions, is also affected by the inclusion content. Figure 5 shows plots of energy absorbed during Charpy v-notch testing as a function of test temperature for 4340 steels tempered to produce either 930 MPa or 1960 MPa strength levels with various sulfur levels[10]. Increasing sulfur indicates an increased volume fraction of MnS inclusions. The figure shows that the upper shelf energy is strongly dependent on the amount of sulfur and thus volume fraction of MnS inclusions, with decreasing upper shelf energy correlating to increased sulfur content. Also of note is that there is no difference in the lower shelf energy and very little difference in the transition temperature as these properties are more correlated to brittle fracture mechanisms such as cleavage, which are not as affected by the inclusion population. Figure 5

also shows that the Charpy impact behavior is much less sensitive to sulfur level when the alloy is heat treated to a higher strength level as the matrix steel is less tough and ductile.

Figure 6 shows results from the same investigation where the upper shelf energy is compared between specimens tested in the transverse and through thickness orientations of the rolled plate (the data in Figure 5 is from the transverse orientation). The through thickness orientation has a lower upper shelf energy and a strong dependence of upper shelf energy on sulfur content, which is associated with the apparent inclusion size on a fracture plane in this orientation as shown in Figure 3 (TD-RD plane).

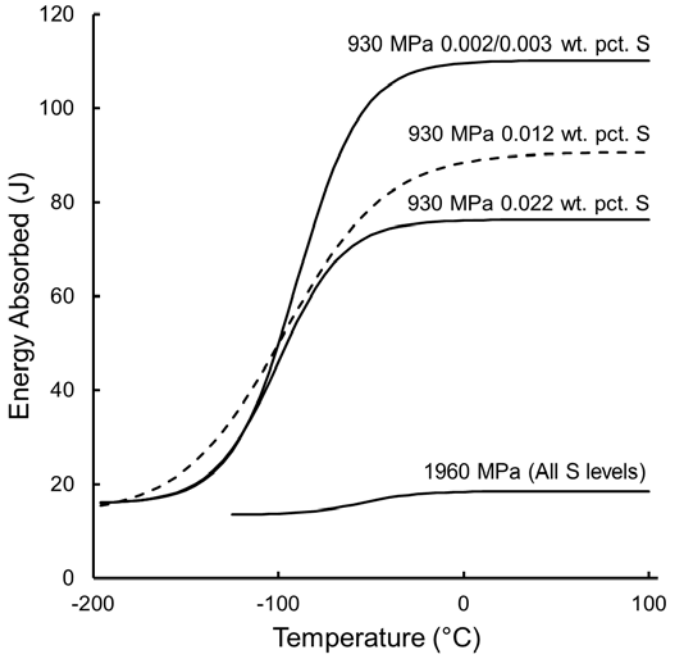

Figure 5: Charpy v-notch data plotted as a function of test temperature for 4340 steel with various sulfur levels heat treated to produce strength levels of 930 MPa or 1960 MPa. Adapted from Speich and Spitzig[10].

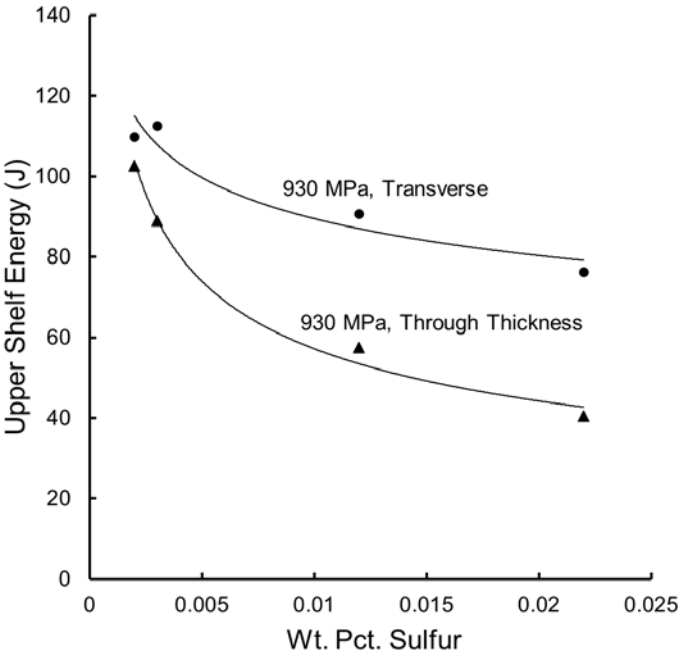

Figure 6: Charpy v-notch upper shelf energy plotted as a function of sulfur content for 4340 steel heat treated to produce a strength level of 930 MPa. Adapted from Speich and Spitzig[10].

The effects of inclusions in rolled or forged materials can be enhanced by microstructural banding and segregation. Deformed inclusions are elongated in the same direction as banding[1]; these bands and segregated regions have composition and microstructure gradients with regions of higher strength and lower toughness separated by lower strength regions of higher ductility.

While inclusions do not have a large influence on brittle fracture, the stress intensity associated with their presence in the matrix can promote cleavage fracture and thus lower both the Charpy ductile to brittle transition temperature and lower shelf energy[12]. This stress intensity is exacerbated by the presence of voids initiated around the inclusion during working, as demonstrated in Figure 2, as these voids serve as starting flaws in the alloy.

THE EFFECTS OF INCLUSIONS ON FATIGUE

The fatigue properties of steel alloys can be influenced by inclusions in both crack nucleation and growth processes. Crack nucleation controlled fatigue lives are governed by the weakest link in the microstructure, which is often inclusions, especially in higher strength steels. The extent that inclusions are the weakest link is again affected by their size, morphology, and the presence of pre-existing voids resulting from previous working. In contrast to toughness, only the largest inclusions affect crack nucleation as these inclusions have the largest stress intensity assuming they are a starting flaw. Extreme value statistical analysis is used to predict the largest inclusions present in an alloy based on the overall inclusion size distribution[13-16].

The crack nucleation process involves inclusions debonding from the matrix, which can happen in one fatigue cycle[17] or during previous working. Thus, inclusion deformability is a critical factor as more deformable inclusions are less likely to debond from the matrix, especially in the presence of small applied strains typical of fatigue loading. Crack nucleation eventually occurs as a result of the stress concentration of the inclusion and localized plasticity[18]. The stress intensity, ΔK, associated with the inclusion can be calculated using the fracture mechanics solution for an internal penny-shaped crack[5]:

$$\Delta K = 0.5 \cdot \sigma_{\max} \sqrt{\pi \sqrt{area}} \qquad \text{Eqn. 3}$$

where σ_{max} is the maximum applied stress and *area* is the cross-sectional area of the inclusion in the plane of fracture. The endurance limit can be calculated as the σ_{max} that results in a ΔK exceeding the threshold stress intensity factor for crack growth, ΔK_{th}, for a given inclusion *area*. A crack nucleation mechanism that competes with inclusions is plastic damage initiated in localized regions of the steel matrix, which is governed by the local yield or critical resolved shear stress. The lower of the two stresses, i.e. the local yield stress and the σ_{max} necessary to exceed ΔK_{th} for a given inclusion area, controls the fatigue crack nucleation process. Since σ_{max} is inversely proportional to inclusion *area*, there is a critical inclusion size where fatigue crack nucleation transitions from being controlled by localized plastic damage to being controlled by inclusions. Figure 7 shows allowable stress as a function of inclusion *area*[19], assuming a ΔK_{th} of approximately 4 MPa*m$^{1/2}$. Also shown is the critical inclusion where crack nucleation mechanism switches to being inclusion controlled as inclusion area increases for several steel alloys. Notably, the critical inclusion area is significantly lower for higher strength grades.

Fatigue crack growth is also affected by the inclusion distribution. Figure 8 shows a plot of fatigue crack growth rate as a function of applied stress intensity range for A533B steel[20]. Specimens were extracted from a hot-rolled plate and tested in different orientations. The curves are labeled with two letters, where the first letter indicates the direction of the applied load and the second indicates the direction of crack propagation. The letters 'S', 'L', and 'T' represent short transverse, longitudinal, and transverse, respectively. For example, the label 'S-L' is for a specimen with an applied load in the short transverse direction and crack growth in the longitudinal direction. The data show that crack growth rates are highest when the load is applied in the short transverse direction and the plane of fracture is in the plane defined by the longitudinal and transverse directions as shown in the schematic in Figure 2. The apparent inclusion size on this fracture plane is larger than the other planes, and thus there is anisotropy in crack growth rates.

While the previous discussion focused on fatigue where there is a resolved tensile stress component, e.g. uniaxial, bending, torsion, inclusions are also important for rolling sliding contact fatigue (RSCF). RSCF is a stress state present in mating gear teeth and on rail steels, for example, and can result in pitting fracture that reduces the functionality of gears. During RSCF, there is a Hertzian contact stress on the specimen or part surface that results in a subsurface shear stress that varies with distance from the surface and reaches a peak at a given subsurface depth depending on the magnitude of the sliding component; the large the sliding component, the closer the peak shear stress is to the surface. Inclusions serve as possible crack nucleation sites in RSCF and since parts subjected to RSCF are typically high strength steels, the critical inclusion size for crack nucleation is relatively small. Figure 9 shows crack nucleation from RSCF damage in a vacuum carburized 4120 steel laboratory RSCF specimen. The image also shows "butterfly" features associated with the crack nucleation process[21]. Thus, inclusion size and volume fraction is also related to RSCF lives[3].

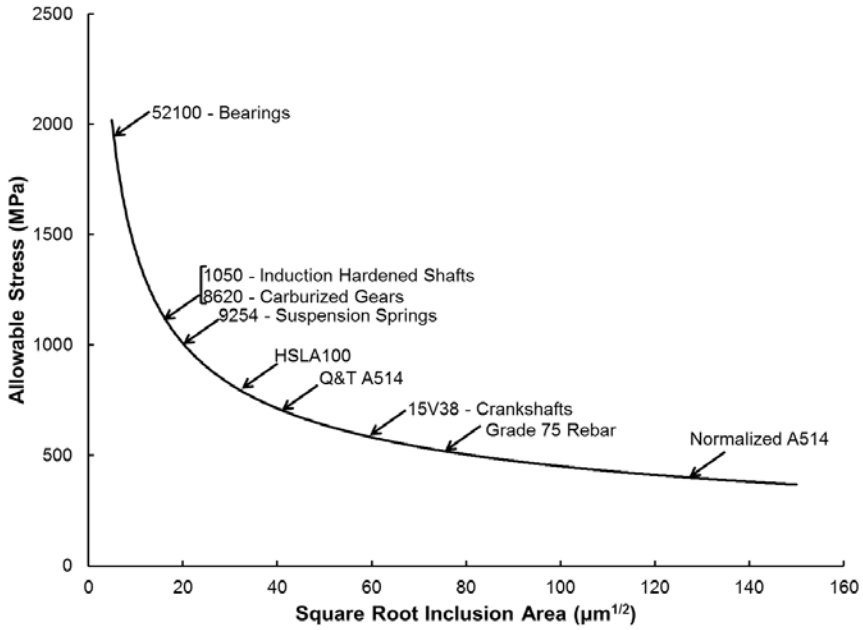

Figure 7: Allowable stress to achieve ΔK_{th} as a function of square root inclusion area with arrows indicating the critical inclusion area where crack nucleation becomes controlled by inclusions[19].

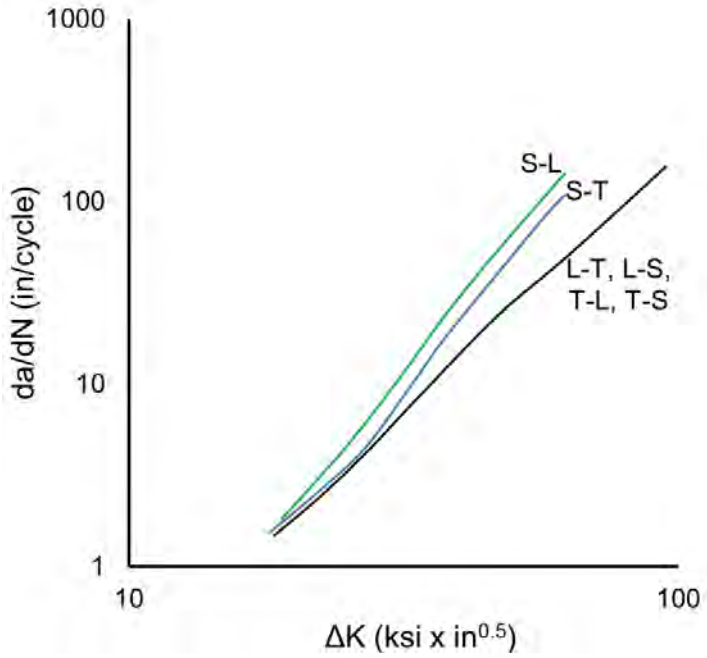

Figure 8: Crack growth rate as a function of applied stress intensity for rolled A533B plate steel tested in different orientations, Adapted from Wilson[20].

THE EFFECTS OF INCLUSIONS ON HYDROGEN EMBRITTLEMENT

Hydrogen embrittlement of steels can occur in a variety of product forms including formed sheets, fasteners, and pipeline steels as examples. Hydrogen diffuses to trapping sites within steel that have varying binding energies. Inclusions have a relatively large binding energy compared to other microstructural features, and hydrogen generally becomes irreversibly trapped at inclusions[22]. Then, hydrogen can facilitate void nucleation at inclusions[22,23] through hydrogen enhanced localized plasticity (HELP)[24], internal pressure as a result of hydrogen combining to form H_2 gas, and reduction of interface energy. Thus, there is reduced ductility in steels containing hydrogen even if the fracture mechanism is ductile; the void nucleation process occurs more readily in the presence of hydrogen, and the inclusion size distribution and volume fraction is important similar to the previous discussion on ductile fracture. The presence of other trap sites such as dislocations can help reduce the interaction of hydrogen and inclusions.

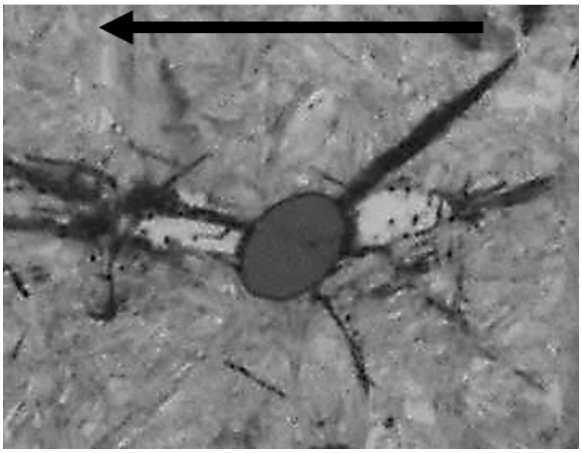

Figure 9: Crack nucleation and "butterfly" formation around an inclusion in a vacuum carburized 4120 steel RSCF specimen[21]. Arrow indicates direction of rolling on the surface.

Hydrogen induced cracking (HIC) is an important subset of hydrogen embrittlement that occurs in pipeline steels in sour environments containing H_2S. HIC occurs when hydrogen diffuses into the pipeline steel and becomes trapped at high energy trap sites such as inclusions, which often are more prominent at the centerline in rolled plates exhibiting alloy segregation[25]. The hydrogen recombines at the inclusion-steel interface to form H_2 gas, which exerts pressure that eventually debonds the inclusion and starts a crack that propagates along the centerline; the centerline is particularly vulnerable because of its higher strength (lower hydrogen embrittlement resistance) and higher fraction of hydrogen trap sites. As the crack grows, hydrogen continues to affect the crack growth process, producing brittle intergranular or cleavage cracking[26]. Steelmaking, hot rolling, and heat treating processes can be designed to control the inclusion size and morphology (i.e. reduce elongation in the rolling direction), reduce segregation, and remove hydrogen from the steel after steelmaking[27].

INCLUSIONS AND MACHINABILITY

During machining, the relative motion between the machining tool and the steel surface results in chip formation, which is the primary mechanism of material removal. Chip formation is a local ductile fracture process involving shear deformation ahead of the cutting tool[28]. Inclusions, especially those that are relatively soft and deformable, can thus enhance machinability by facilitating ductile fracture. It has been shown that void formation preferentially occurs at the inclusion-steel interface during chip formation[29]. However, hard particles are not desired for machinability because they can reduce tool life through surface abrasion.

Lead particles can lubricate the interface between the cutting tool and chip during machining, providing another enhancement to machinability. However, lead inclusions have been largely removed from steel products because of environmental factors, and other alloying elements[30,31] and alloying and processing to produce graphitization[32] have been explored as alternatives.

SUMMARY AND CONCLUSIONS

Many aspects of the mechanical behavior of steel components are strongly dependent on the inclusion population in a wide variety of steel alloys and products. Therefore, steelmaking and processing considerations are critical in the ultimate role inclusions have on properties. For example, rolled plates can exhibit anisotropic properties due to pancaking and elongation of inclusions. In this paper, the effects of inclusions on ductile fracture, fatigue, hydrogen embrittlement, and machinability are highlighted. However, this discussion of effects of inclusions on properties is not comprehensive, and several references have been cited that provide further information.

REFERENCES

1. S. Abraham, S. Seetharaman, B. Jones, "Types and Origins of Non-Metallic Inclusions", Peaslee Inclusion Engineering and Clean Steel Commemorative Volume, 2017.
2. R.J. Fruehan, Ladle Metallurgy Principles and Practices, ISS, Warrendale, PA, 1985.
3. W.C. Leslie, "Inclusions and Mechanical Properties," Mechanical Working and Steel Processing XX, 1982, pp. 3-50.
4. T.M. Banks, T. Gladman, "Sulphide shape control," Metals Technology vol. 6, 1979, pp. 81-94.
5. Y. Murakami, Metal Fatigue: Effects of Small Defects and Nonmetallic Inclusions, Elsevier, Amsterdam, Netherlands, 2002.
6. C.G. Glenn, The Effects of Ti, Zr, and Al Nitrides on Ductile Fracture in Thin Plates of Hardened 0.3C Steels, M.S. Thesis, Colorado School of Mines, 1989.

7. W.M. Garrison, “Controlling Inclusion Distributions to Achieve High Toughness Steels,” AIST Transactions, vol. 4, 2007, pp. 132-139.
8. W.M. Garrison, A.L. Wojcieszynski, “A discussion of the effect of inclusion volume fraction on the toughness of steel,” Materials Science and Engineering A, vol. 464, 2007, pp. 321-329.
9. M.G. Hebsur, K.P. Abraham, Y.V.R.K. Prasad, “Influence of Electroslag Refining on the Hot Ductility of AISI 4340 Steel in Tension,” Journal of Mechanical Working Technology, vol. 4, 1981, pp. 341-349.
10. G.R. Speich, W.A. Spitzig, “Effect of Volume Fraction and Shape of Sulfide Inclusions on Through-Thickness Ductility and Impact Energy of High-Strength 4340 Plate Steels,” Metallurgical Transactions A, vol. 13A, 1982, pp. 2239-2258.
11. R.A. Grange, “Effect of Microstructural Banding in Steel,” Metallurgical Transactions A, vol. 2, 1971, pp. 417-426.
12. M.A. Linaza, J.M. Rodriguez-Ibabe, J.J. Urcola, “Determination of the Energetic Parameters Controlling Cleavage Fracture Initiation in Steels,” Fatigue and Fracture of Engineering Materials and Structures, vol. 20, 1997, pp. 619-632.
13. S. Beretta, C. Anderson, Y. Murakami, “Extreme Value Models for the Assessment of Steels Containing Multiple Types of Inclusions,” Acta Materialia, vol. 54, 2006, pp. 2277-2289.
14. C. Barbosa, J. Brant de Campos, J. Lopes do Nascimento, I. Caminha, “Quantitative Study on Nonmetallic Inclusion Particles in Steels by Automatic Image Analysis with Extreme Values Method,” Journal of Iron and Steel Research, vol. 16, 2009, pp. 18-21.
15. E.B. Damm, P.C. Glaws, “Gear Design Relevant Cleanness Metrics,” American Gear Manufacturers Assocation, 2016.
16. A.B. Nissan, K. O. Findley, A. S. Hering, "Extreme value statistical analysis to determine the endurance limit of a 1045 induction hardened steel alloy," Procedia Engineering, vol. 10, 2011, pp. 607-612.
17. J. Lankford, “Inclusion-Matrix Debonding and Fatigue Crack Initiation in Low Alloy Steel,” International Journal of Fracture, vol. 12, 1976, pp. 155–157.
18. K. Tanaka and T. Mura, “A Theory of Fatigue Crack Initiation at Inclusions,” Metallurgical and Materials Transactions A, Vol. 13, 1982, pp. 117–123.
19. K.O. Findley, R.L. Cryderman, A.B. Nissan, D.K. Matlock, “The Effects of Inclusions on Fatigue Performance of Steel Alloys,” AIST Transactions, vol. 10, 2013, pp. 234-244.
20. A.D. Wilson, "The Influence of Inclusions on the Toughness and Fatigue Properties of A516-70 Steel," Journal of Engineering Materials and Technology, vol. 101, 1979, pp. 265-274.
21. P. Kramer, An Investigation of Rolling-Sliding Contact Fatigue Damage of Carburized Gear Steels, M.S. Thesis, Colorado School of Mines, 2013.
22. R.A. Oriani, “Hydrogen Embrittlement of Steels,” Annual Review of Materials Science, vol. 8, 1978, pp. 327-357.
23. J.P. Hirth, “Effects of Hydrogen on the Properties of Iron and Steel,” Metallurgical Transactions A, vol. 11A, 1980, pp. 861-890.
24. I.M. Robertson, “The Effect of Hydrogen on Dislocation Dynamics,” Engineering Fracture Mechanics, vol. 68, 2001, pp. 671-692.
25. G. Domizzi, G. Anteri, J. Ovejero-Garcia, “Influence of sulphur content and inclusion distribution on the hydrogen induced blister cracking in pressure vessel and pipeline steels,” Corrosion Science, vol. 43, 2001, pp. 325-339.
26. K.O. Findley, M.K. O’Brien, H. Nako, “Critical Assessment 17: Mechanisms of hydrogen induced cracking in pipeline steels,” Materials Science and Technology, vol. 31, 2015, pp. 1673-1680.
27. J. Nieto, T. Elias, G. Lopez, G. Campos, F. Lopez, R. Garcia and A. K. De, “Development of technology for the production of HIC resistant slabs for sour service applications at Arcelormittal Lazaro Cardenas Mexico,” Proceedings of Materials Science and Technology, 2012, pp. 1044–1053.
28. J.T. Black, “Mechanics of Chip Formation,” ASM Handbook Volume 16, Machining, 1989, pp. 7-12.
29. L. Sidjanin, P. Kovac, “Fracture mechanisms in chip formation processes,” Materials Science and Technology, vol. 13, 1997, pp. 439-444.
30. J. G. Speer, D.K. Matlock and G. Krauss, "Recent Developments in the Physical Metallurgy of Ferrous Long Products", Transactions of the Indian Institute of Metals, Vol.59, 2006, pp.749-767.
31. D. Bhattacharya, D.T. Quinto, "Mechanism of hot-shortness in leaded and tellurized free-machining steels," Metallurgical Transactions A, vol. 11, 1980, pp. 919-934.
32. K. He, H. R. Daniels, A. Brown, R. Brydson, D. V. Edmonds, "An electron microscopic study of spheroidal graphite nodules formed in a medium-carbon steel by annealing," Acta materialia, vol. 55, 2007, pp. 2919-2927.